SIZE EFFECT ON MASONRY SUBJECTED TO OUT-OF-PLANE LOADING

P.B. Lourenço, J.A.O. Barros

ABSTRACT

Size effect is a key aspect of masonry mechanics. This salient feature of quasi-brittle materials, which is mostly governed by the post-peak behavior of masonry and not by the randomness of the material strength, has been adopted in concrete codes but not in the new European code – Eurocode 6. In this paper, theoretical and experimental evidence of size effect in masonry subjected to flexure is presented, demonstrating the need of defining the flexural strength as a function of the width of the masonry wall.

KEYWORDS

Flexural tensile strength, size effect, softening, randomness

1. INTRODUCTION

Until about a decade ago, it was generally believed that the size effect in structural failure was of statistical origin, caused by the randomness of material strength, particularly by the fact that in a larger structure it is more likely to encounter a material point of smaller strength. Accordingly, it was thought that studies of the size effect should be left to statisticians and that the size effect should be relegated to the safety factor.

Recently, however, it has been discovered that an important and often dominant size effect can be of purely mechanical and deterministic origin. Whenever failure does not occur at the initiation of cracking, which represents most situations in quasi-brittle materials, the size effect should be properly explained by energy release caused by macro-crack growth and the randomness of strength plays only a negligible role, Bazant and Xi (1991). The proper explanation of size effect has been shown to lie in the release of strain energy due to fracture growth, producing damage localization instabilities. Prior to failure, distributed damage, consisting principally of micro-cracking, localizes into a narrow fracture process zone, which ultimately becomes the final, major crack. The localization is driven by the release of stored strain energy from the structure. In a larger structure, the strain energy is released from a larger zone and so the total amount that would be released for a unit crack advance would be larger if the nominal stress was the same. However, because the energy required to produce a unit fracture extension is approximately independent of the structural size, the nominal stress at failure of a larger structure must be lower, so that the energy release matches the fracture energy.

Thus, such a size effect can be caused by the influence of the release of the stored elastic energy on the nominal strength of the structure. Many studies, both of experimental and theoretical nature, have already dealt with this type of size effect, and an approximate size-effect law applicable to structures in which fracture is preceded by distributed cracking in a large fracture-process zone has been formulated already by Bazant (1984). A comprehensive study on the evidence of fracture size effect for concrete structures and a comparison with extensive experimental data can be found in Bazant *et al* (1994).

Department of Civil Engineering, School of Engineering, University of Minho, Azurém, P - 4800-058 Guimarães, PORTUGAL • Tel.: +351 253 510200 • Fax: +351 253 510217 • E-mail: pbl@eng.uminho.pt

The problem of size effect is particularly important to structural and geotechnical engineers, who must inevitably extrapolate from reduced-scale laboratory tests to real structures, which are too large to be tested systematically. For masonry structures, additionally, tests performed using units with one half the real size, Page (1981), one quarter of the real size, Gergely *et al* (1993), up to one sixth of the real size, Samarasinghe and Hendry (1980), are common. Here, we address the particular case of size effect on the flexural bond strength of masonry, introducing the theoretical aspects and experimental evidence. From these results, it is clear that masonry bond flexural strength depends on the masonry unit width and cannot be considered a material property.

2. ASPECTS OF THE FLEXURAL BEHAVIOR

There has been much work done about the flexural tensile strength of masonry along the two principal material directions. Nevertheless, moment-curvature diagrams are normally lacking and very little work was carried out on size effect, namely, in the consequences of the variability of material properties and of softening behavior (real tensile strength vs. measured flexural strength).

It has been (and it still is) common practice to perform bending tests to describe structures subjected to out-of-plane forces. This is mostly done due to practical reasons, as bending tests are relatively easy to carry out, e.g. three-point bending, four-point bending or the bond-wrench test proposed by Hughes and Zsembery (1980), see Figure 1. No discussion is given here about different test set-ups and the reader is referred to van der Pluijm (1996) for a modern discussion on measuring flexural bond strength. A comprehensive review about flexural properties of masonry is given in Lawrence (1983), including the adequacy of testing methods and the reliability of results. Particular attention is given there to the influence in the results of secondary effects (such as non-ideal supports), lack of displacement and strain data, variability of properties, workmanship and age of testing.

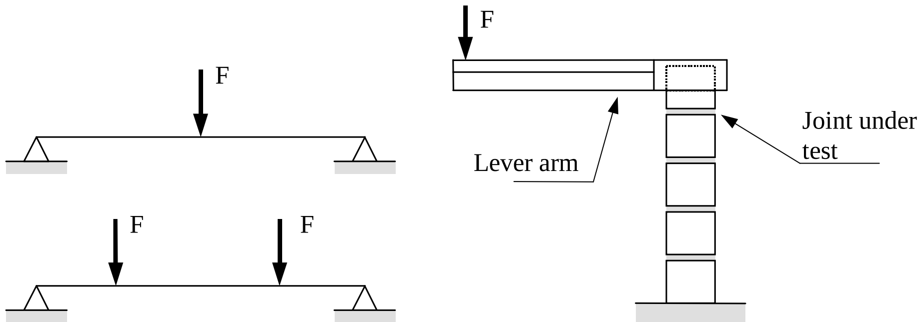

Figure 1 - Examples of tests to obtain the tensile flexural strength of masonry: three-point bending, four-point bending and bond-wrench test

The flexural strength of masonry has been mostly investigated in relation to the resistance of wall panels to wind loads. The flexural strength is, of course, different for bending perpendicular or parallel to the bed joints, see Figure 2, being normally several times larger when bending leads to failure in a plane perpendicular to the bed joints. In general, experimental results have been concerned solely with measurements of the flexural strength and mostly for the case when the plane of failure occurs parallel to the bed joints, while elastic and inelastic properties have usually been ignored.

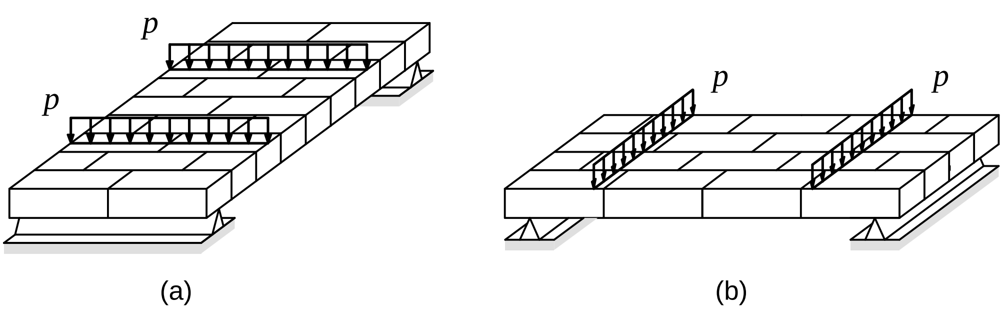

Figure 2 - Four-point bending test in two different directions: (a) plane of failure parallel to the bed joints - *vertical bending or bending normal to the bed joints* - and (b) plane of failure perpendicular to the bed joints - *horizontal bending or bending parallel to the bed joints*

For bending leading to failure in a plane parallel to the bed joints (“vertical bending”), failure is generally caused by the relatively low tensile bond strength between the bed joints and the unit, see Figure 3a. In masonry with low strength units and greater tensile bond strength between the bed joints and the unit, e.g. high-strength mortar and units with numerous small perforations, which produce a dowel effect, failure may occur as a result of stresses exceeding the unit tensile strength. In any case, the typical moment-curvature relation is linear up to 70%-85% of the failure load, Lawrence (1983) and van der Pluijm et al (1995), see Figure 4a. Beyond this level micro-cracking starts to occur, with unloading (“softening”) of the extreme tensile fibers.

For bending leading to failure in a plane perpendicular to the bed joints (“horizontal bending”), two different types of failure are common, depending on the relative strength of joints and units, see Figure 3b. In the first type of failure cracks zigzag through head and bed joints. The post-peak response of the specimen is governed by the fracture energy of the head joints and the friction behavior of bed joints. In the second type of failure cracks run almost vertically through the units and head joints. The post-peak response is governed by the fracture energy of the units and head joints. In both types of failure, the typical moment-curvature relation indicates a sudden decrease of stiffness before non-linear behavior starts to occur, see Figure 4b. This kind of behavior was originally noticed by Ryder (1963). Lawrence (1983) attributed this behavior to the gradual decrease of stiffness of the head joints, i.e. the softening behavior, which has been confirmed by van der Pluijm et al (1995). It is noted that the above holds true only in the general case of units with a tensile strength substantially larger than the tensile strength of the head joints.

Here, only the latter case will be addressed, which represents, in fact, a discussion on the flexural bond strength of masonry.

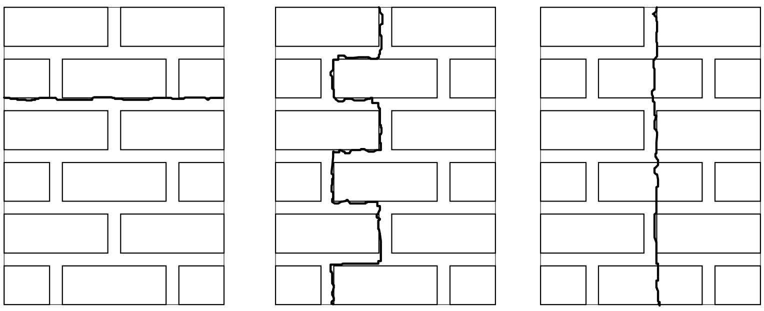

(a) (b1) (b2)

Figure 3 - Possible failure modes for masonry subjected to bending along the material axes. Failure in a plane parallel to the bed joints: (a) “debonding”. Failure in a plane perpendicular to the bed joints: (b1) “toothed” and (b2) “splitting”

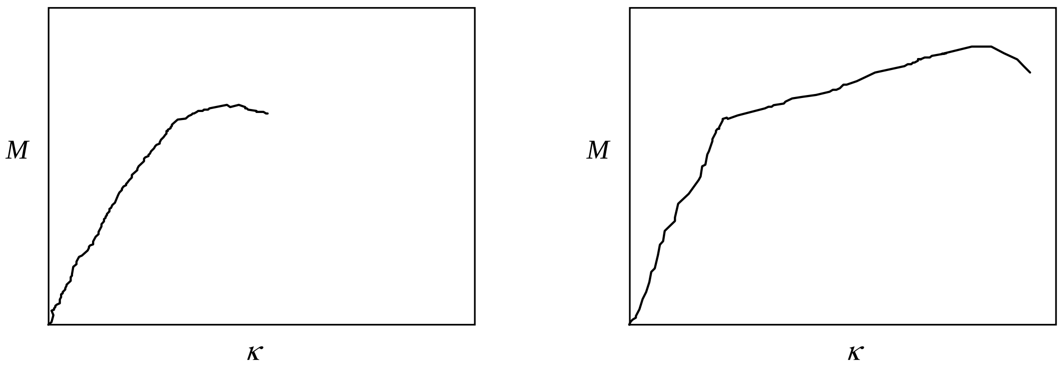

(a) (b)

Figure 4 - Typical moment-curvature (M-κ) diagrams for masonry in bending such that failure occurs in a plane (a) parallel and (b) perpendicular to the bed joints

3. SIZE EFFECT AND THE RANDOMNESS OF MATERIALS

As a result of many studies, it has been shown that brittle failure of concrete structures exhibits a size effect. For a long time, the size effect has been explained statistically as a consequence of the randomness of the material, particularly by the fact that in a larger structure it is more likely to encounter a material point of smaller strength. Various existing test data were interpreted in terms of Weibull weakest-link theory. Later, it was proposed by Bazant (1984) that whenever the failure does not occur at initiation of cracking, which represents most situations, the size effect should properly be explained by energy release caused by macro-crack growth, and that the randomness of strength plays only a negligible role. Presently, the role of the softening behavior is accepted by all the scientific community to explain size effect.

In the next section, the direct consequence of softening in the flexural strength of masonry will be discussed. Now, we address the problem of randomness of strength in masonry structures which seems to play a crucial role in size effect, Lawrence (1983). This effect, which is due to a much higher coefficient of variation, seems to have been firstly taken in consideration for masonry structures by Baker and Franken (1976), with respect to the flexural strength of brickwork. Of course, this is not only a problem for the flexural strength but in all failures related to the tensile strength (size effect due to “crushing” is more complex and will not be discussed here). Remarkably, the subject received a lot of publicity in relation to flexural strength and very little with relation to tensile strength! This seems to confirm a certain incipient knowledge of masonry structures.

From the test results, e.g. Lawrence (1983) and van der Pluijm (1996), it is essential to treat a masonry beam as being composed of a number of discrete joints, each with a different strength. This is due to the high variability in masonry properties and the softening behavior which leads to localization of deformation in a single joint and unloading of the rest of the specimen. Because failure of each single joint leads to failure of the whole beam, a weakest-link theory has to be adopted. The theory of order statistics will not be reviewed here but, for a given distribution of joint strengths (which must be approximately normal), the mean $\bar{f}_{ft,beam}$ and standard deviation $\sigma_{ft,beam}$ of the beam strength can be obtained from the mean $\bar{f}_{ft,joint}$ and standard deviation $\sigma_{ft,joint}$ of the joint strength, from the following relations:

$$\begin{cases} \bar{f}_{ft,beam} = \bar{f}_{ft,joint} - k_1 \times \sigma_{ft,joint} \\ \sigma_{ft,beam} = k_2 \times \sigma_{ft,joint} \end{cases} \tag{1}$$

where the values of k_1 and k_2 depend on the number of joints and can be found in e.g. Mosteller and Rourke (1973), see Table 1.

Table 1 - Weakest-link theory coefficients, Mosteller and Rourke (1973)

No. of joints	2	3	4	5	6
k_1	0.56	0.85	1.03	1.16	1.27
k_2	0.826	0.748	0.696	0.669	0.645

Figure 5 shows clay brick specimens tested in vertical bending, van der Pluijm (1996). Table 2 shows the results obtained in the different tests, which demonstrate the need of a correction. The mean flexural strength, in the single joint, is 0.66 N/mm^2 and, in the wallettes, is 0.56 N/mm^2 (85%). The standard deviation, in a single joint, is 0.20 N/mm^2 and, in the wallettes, is 0.16 N/mm^2 (80%).

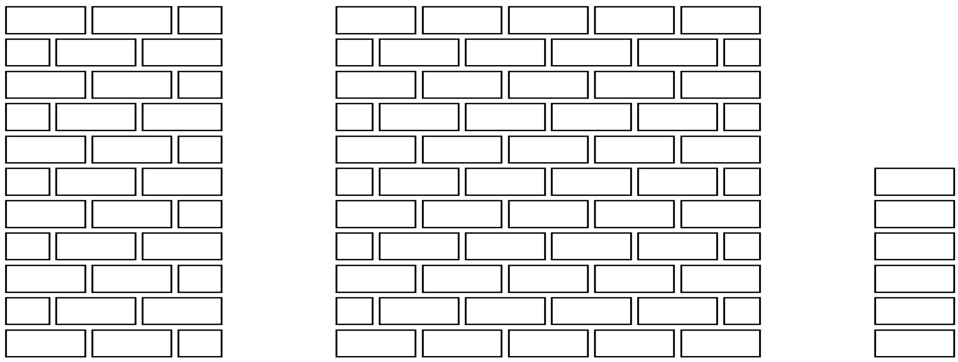

(a) (b) (c)

Figure 5 - Clay brick specimens: (a) normal wallette, (b) double width wallette and (c) stacked bonded pier, van der Pluijm (1996)

Table 2 - Average strength and coefficient of variation for flexural strength value according to three different specimens, van der Pluijm (1996)

	single joint (pier)	single joint (bond wrench)	normal wallettes	double width wallettes
f_{ft} [N/mm^2]	0.64	0.68	0.57	0.56
c.v. [%]	30	29	29	27

The weakest-link theory gives a ratio of 70% (four joints in pure flexure), both for the mean and the standard deviation. A cause for this outcome is not perfectly clear but it is questionable to use eq. (1), with the parameters of Table 1, in this case because the pier has a width of one unit and the wallettes have a larger width. Due to the manufacturing and curing processes different statistical distribution of strengths will be found in the pier joint and the wallette joint. A better agreement between the weakest-link theory and tests can be found in Lawrence (1983).

The randomness of material properties will be ignored in this paper. It is noted that a large masonry structure is normally subjected to quite non-uniform stress conditions. Therefore, collapse will result from failure in a large number of joints and the panel failure mode is heavily constrained by the boundary conditions. This means that averaging effects are likely to occur, i.e. randomness of properties becomes less important.

4. SIZE EFFECT AND THE SOFTENING BEHAVIOR

The size effect is defined by comparing the nominal strength (nominal stress at failure) σ_N of geometrically similar structures of different sizes. For two-dimensional (2D) similarity, $\sigma_N = c_n F_u / (b.d)$, and for three-dimensional similarity, $\sigma_N = c_n F_u / d^2$, where F_u is the maximum (ultimate) load of the structure, b is the structural thickness, d is the characteristic dimension (size), which may be introduced as any dimension of the structure (for example beam depth), and c_n is any given coefficient introduced for convenience. One may set $c_n = 1$, or may use c_n such that σ_N would coincide with some convenient stress formula. For example, in the case of a simply supported beam of span L and a rectangular cross section of depth H, loaded at mid-span, one may set $d = H$ and $c_n = 3L / 2H$, in which case $\sigma_N = 3F.L / (2b.H^2)$ = maximum elastic bending stress (note that L/H and b are constant for 2D similarity).

The size effect is understood as the dependence of σ_N on the structure size d (characteristic dimension). According to the plastic limit analysis, as well as any theory in which the material failure is characterized in terms of stresses or strains, σ_N is independent of the structural size, i.e. there is no size effect (this may be illustrated, e.g., by the elastic or plastic formulas for beams subjected to bending, shear or torsion). In linear elastic fracture mechanics, in which all the fracture process is assumed to occur at a point - the crack tip - σ_N declines in proportion to $d^{-½}$. This means that the plot of Log(σ_N) versus Log(d) (Figure 6) is an inclined straight line of slope –½ , provided that the cracks at the moment of failure of structures of different sizes are geometrically similar. Note that the similarity of cracks at failure has been experimentally demonstrated for most, though not all, types of failures of concrete structures of different sizes, in the usual size range. No such information is available for masonry structures.

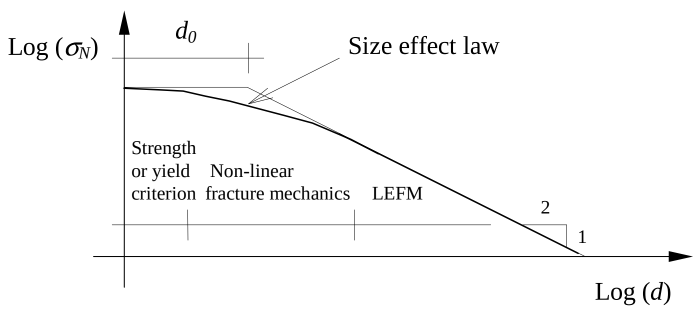

Figure 6 - Size effect law proposed by Bazant (1984)

In concrete structures, the size effect is transitional between the strength (or yield) criterion (i.e. no size effect), represented by the horizontal line in Figure 6, and the size effect of linear elastic fracture mechanics, represented by the inclined straight line in Figure 6. For most practical purposes, this curve can be described by the size effect law, Bazant (1984),

$$\sigma = \left(A + B\,d\right)^{-1/2} \quad (2)$$

in which A and B are two constants determined either experimentally or by a more sophisticated analysis (e.g. using a finite element code that is able to realistically predict softening and failure process in quasi-brittle materials).

For $d << d_0$, eq. (2) yields $\sigma_N = B$ = constant, which means that the size effect disappears. For $d >> d_0$, eq. (2) yields $\sigma_N = B.\beta^{-½}$, which gives the straight line in Figure 6 of downward slope –½ . Thus, the asymptotes of the size effect law are the plastic limit analysis and the linear elastic fracture mechanics. Obviously, structures of sizes $d > d_0$ are predominantly brittle and structures with $d < d_0$ are predominantly ductile.

The reason for this law is that the energy consumed by fracture in structures geometrically similar in two dimensions is proportional to the structure size, whereas the energy released by fracture at the same nominal stress is proportional to structure size squared. As discussed above, contrary to the general opinion a dozen years ago, the Weibull-type statistical size effect due to randomness of material strength is insignificant for failures occurring after large stable crack growth. The reason is that the fracture process zone has about the same size for structures of different sizes. The statistical size effect is important only when failure occurs immediately at crack initiation from a small flaw, but most structures are designed to avoid such failures.

It is noted that the original size effect law of Bazant (1984) was formulated for notched specimens, scaled proportionally to the structural size. For non-notched specimens an additional cut-off is needed because even the largest members, without an initial crack (induced, for example, by a notch), have a non-zero failure load, on the contrary to the predictions of the above law.

4.1 Size effect and the concept of flexural strength

Two arguments have been presented in favor of using bending tests (three-point or four-point bending) to obtain the flexural strength of a material. Firstly, the tests are relatively easy and inexpensive to perform and, secondly, if one is dealing with plates and shells it seems natural to directly characterize the bending tests behavior. Nevertheless, one question that arises in practice is the relation between tensile and flexural strengths.

In the following, it is assumed for simplicity that only tensile inelastic behavior occurs in the structure. For a cross section of a beam or plate in pure bending, see Figure 7, the elementary linear elastic beam theory yields a tensile flexural strength

$$f_{ft} = \frac{6M_u}{bh^2} \quad (3)$$

where f_{ft} is the flexural tensile strength, M_u is the ultimate (*elastic*) bending moment, and b, h are the dimensions of the cross section of the beam.

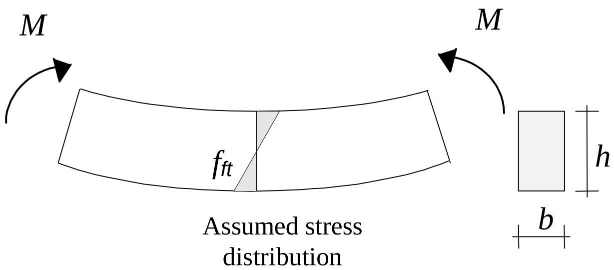

Figure 7 - Beam under pure bending. Linear elastic theory

But the value given from eq. (3) is not the real uniaxial tensile strength. If the beam is subjected to increasing load, at a certain stage the tensile strength of the extreme fiber will be reached. The stress in this fiber starts to follow the descending branch, the micro-crack propagates upwards and the neutral axis of the cross section shifts towards the fibers in compression. Although micro-cracking is occurring, the bending moment can still be increased until the peak moment is reached. Only at the ultimate stage, a fully developed crack occurs. The internal stress distribution in the cross section through all the process is shown in Figure 8.

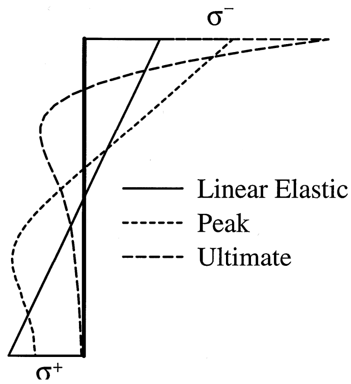

Figure 8 - Normal stress distribution in a cross-section subjected to pure bending

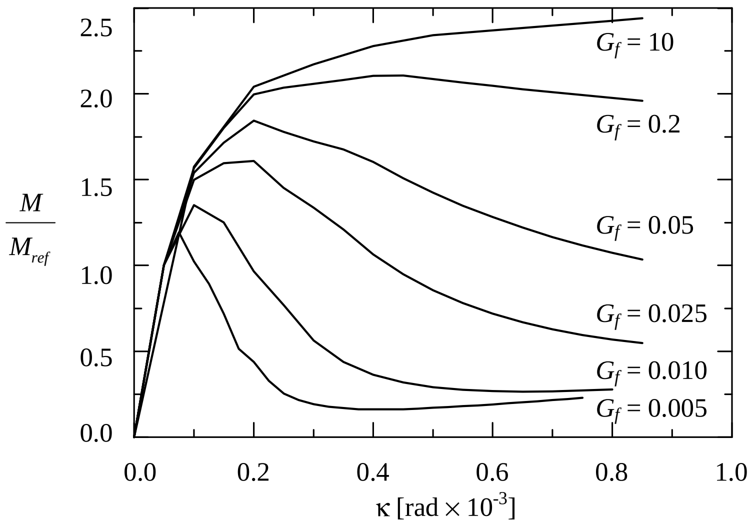

(a)

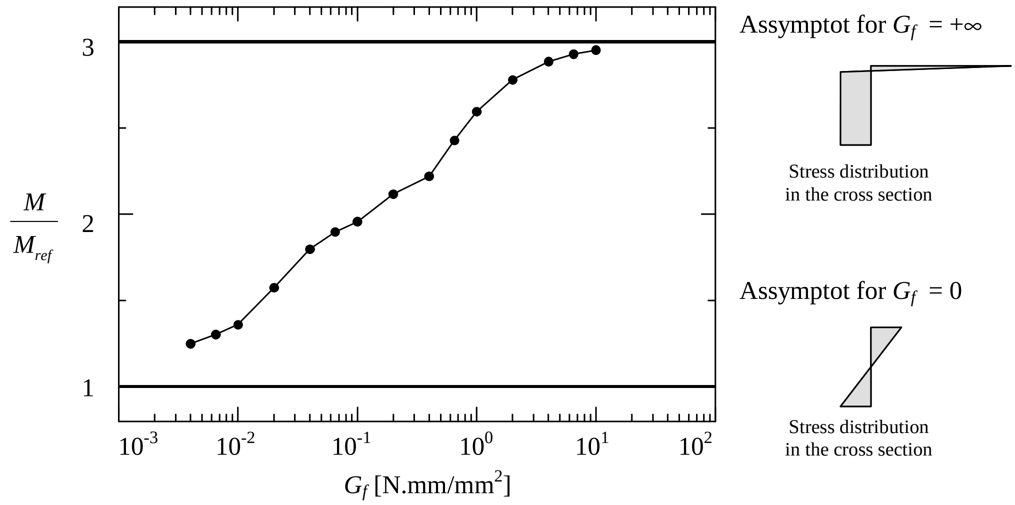

(b)

Figure 9 – Influence of the fracture energy, measured in N.mm/mm^2, on (a) moment-curvature (M-κ) diagram and (b) value of maximum bending moment. The uniaxial strength is kept constant.

The conclusion that the ultimate moment by itself is not enough to determine the constitutive behavior of masonry is crucial. In particular, it means that most of the experimental out-of-plane results in masonry specimens are of limited interest. A complete material characterization derived from bending tests has to include the ultimate moment (directly related to the flexural tensile strength) and the moment-curvature diagram. These “quantities” permit a description at constitutive level based on the (real) tensile strength and the fracture energy G_f, where G_f represents the area under the uniaxial tensile stress-crack_displacement diagram.

In the following example, the real uniaxial tensile strength f_t is kept constant (equal to 3 N/mm^2), while the fracture energy is varied from a very low value to a very high value. If the fracture energy is zero, failure occurs once the extreme fiber reaches the maximum tensile stress, i.e. a linear distribution of stresses is obtained at collapse. The correspondent ultimate moment, denoted by M_{ref} (reference), can be directly obtained from eq. (3). In all other case, this relation is incorrect and its use is debatable. Figure 9 shows the significant influence of the fracture energy G_f in the moment-curvature diagrams and the ultimate bending moment. As the value of the ultimate bending moment can, in theory, be magnified by a factor three, it does not provide a reliable basis to estimate both the real uniaxial strength and the fracture energy.

In masonry specimens, very little research has been carried out regarding this aspect but, it is obvious, that the influence of the descending branch of the stress-crack width diagram diminishes with increasing height h of the cross-section. As an example, for concrete, the Model Code 90, CEB (1993), provides the following expression

$$f_t = f_{ft} \frac{1.5(h/h_0)^{0.7}}{1+1.5(h/h_0)^{0.7}} \qquad (4)$$

where f_t is the uniaxial tensile strength, h_0 equals 100 mm and the height of the cross section h is expressed in mm.

4.2 Experimental Results

In order to demonstrate the size effect of masonry subjected to out-of-plane loading, a number of tests were carried out on aerated concrete block masonry. For this purpose, a typical three-point loading set-up was prepared, see Figure 10. The height h of the specimens assumed the values of 100, 150, 200, 240 and 300 mm. Four specimens of each height h were made, resulting in a total of twenty tests.

The typical force-displacement at mid-span diagram is illustrated in Figure 11 for a height h of 100 mm. Due to smooth face of the aerated concrete block, the very brittle response in the post-peak range could not be traced. Table 3 shows the results in terms of maximum bending moment, resulting from the applied load and the self weight of the specimen, and flexural tensile strength of the specimen, calculated from eq. (3).

A reduction in the flexural tensile strength is clearly visible in the tests. The reduction is shown graphically in Figure 12, both in standard and logarithmic scales. It is noted that:

- Convergence for a minimum strength value upon size increase could not be found – this result can be considered normal as the maximum height of the specimens (300 mm) seems to be too small for reaching collapse at the onset of cracking in the most extreme fiber;

- In the logarithmic scale, the reduction of strength follows an approximately linear law, as defined above;

- In the logarithmic scale some deviation is found for the smallest height (100 mm) – the deviation is probably due to the fact that, for these specimens, the flexural strength measured is not the bond strength but the unit strength, see Figure 13. In fact, the increase of the measured flexural strength associated with the reduction of size led to failure of the unit, instead of the joint. Therefore, this result should be ignored in a size effect analysis.

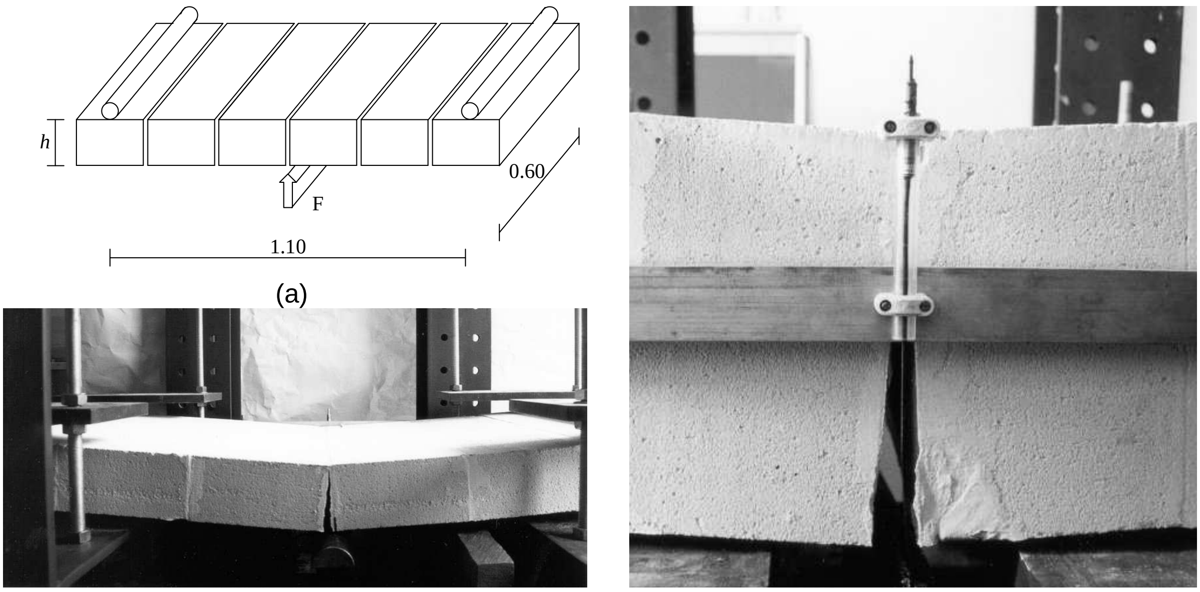

(b) (c)

Figure 10 – Three-point loading: (a) geometry, (b) test set-up and (c) displacement transducer

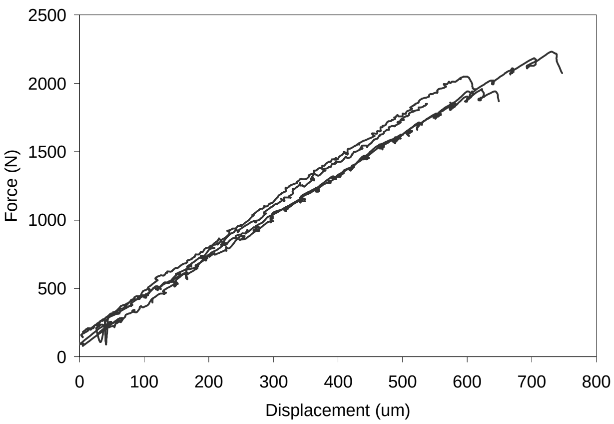

Figure 11 – Force-displacement at mid-span diagram for a height *h* of 100 mm (four specimens)

Table 3 – Average maximum bending moment and flexural strength for all the specimens

h (mm)	100	150	200	240	300
M (KN.mm/mm)	1.18	2.43	3.74	4.97	6.96
f_{ft} (N/mm^2)	1.18	1.08	0.94	0.86	0.77

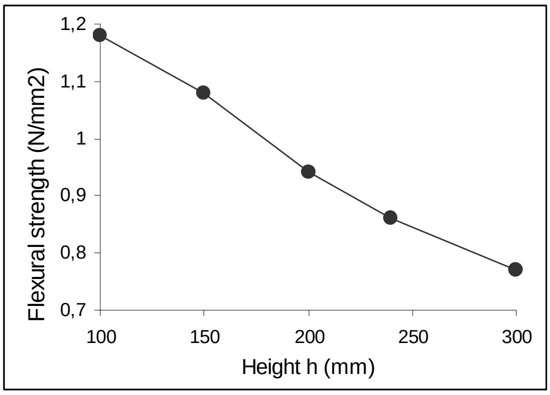

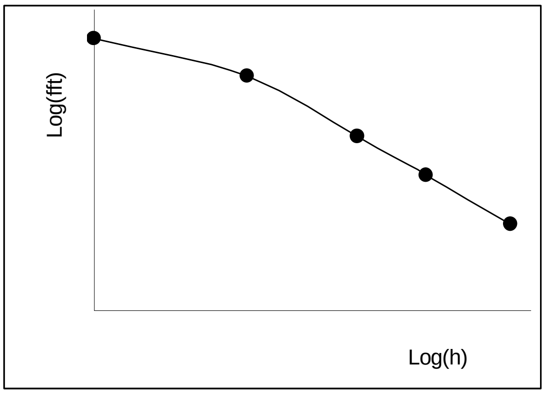

(a) (b)

Figure 12 – Size effect results on the flexural bond strength: (a) standard and (b) logarithmic scales

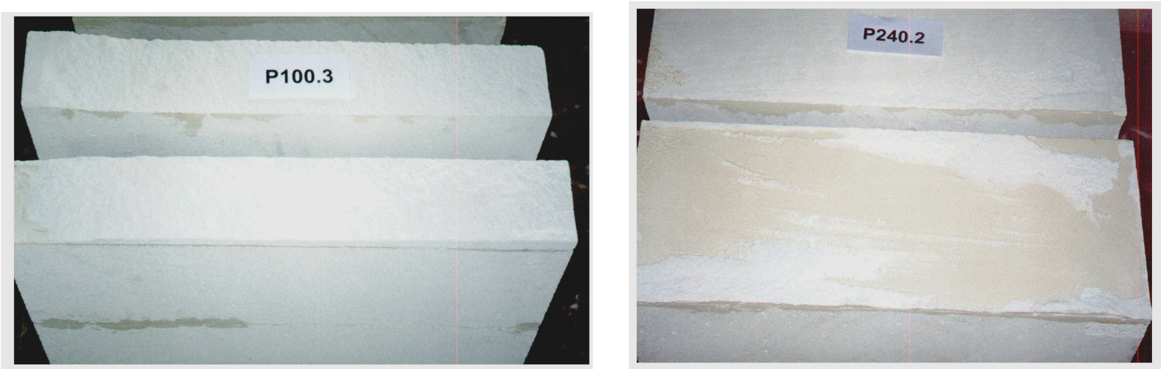

(a) (b)

Figure 13 – Aspects of the failure surface for different height of the wall: (a) 100 mm and (b) 240 mm

5. CONCLUSIONS

A brief review on the uniaxial flexural behavior of masonry has been presented and the dependence of the results on the size of the specimen has been addressed. The aspects of randomness of material properties and post-peak behavior of the stress-strain uniaxial tensile response have been presented.

Theoretical and experimental evidence of size effect on the flexural bond strength of masonry have been presented, as a result of the quasi-brittle behavior of the material. This demonstrates the need to include provisions in the masonry codes for making the flexural strength dependent on the specimen height (or unit width).

REFERENCES

Baker, L.R., Franken, G.L. (1976) - Variability aspects of the flexural strength of brickwork, in: Proc. Forth Int. Brick Mas. Conf., Brussels, Belgium.

Bazant, Z.P. (1984) - Size effect in blunt failure: concrete, rock, metal, J. Engrg. Mech., ASCE, 110(4), p. 518-535.

Bazant, Z.P., Xi, Y. (1991) - Statistical size effect in quasi-brittle structures, J. Engrg. Mech., ASCE, 117(11), p. 2609-2640.

Bazant, Z.P., Ozbolt, J., Eligehausen, R. (1994) - Fracture size effect: review of evidence for concrete structures, J. Struc. Mech., ASCE, 120(8), p. 2377-2398.

CEB (1993) - CEB-FIP Model code 1990: Design code. Thomas Telford, London.

Gergely, P., White, R.N., Zawilinski, D., Mosalam, K. (1993) - The interaction of masonry in-fill and steel or concrete frames, Proc. 1993 Nat. Earthquake Conf., USA, Vol. 2, p. 183-191.

Hugues, D.M., Zsembery, S. (1980) - A method of determining the flexural bond strength at right angles to the bed joint, in: Proc. Second Canad. Mas. Symp., Ottawa, Canada, p. 73-86.

Lawrence, S.J. (1983) - Behaviour of brick masonry walls under lateral loading, Dissertation, School of Civil Engineering, University of New South Wales, Australia.

Mosteller, F., Rourke, R.E.K. (1973) - Sturdy statistics (non-parametrics and order statistics), Addison-Wesley, Reading, Massachusetts, USA, (Appendix A).

Page, A.W. (1981) - The biaxial compressive strength of brick masonry, Proc. Instn. Civil Engrs., Part 2, 71, p. 893-906.

van der Pluijm, R. (1996) - Measuring of bond: A comparative experimental research, in: Proc. Seventh North Amer. Mas. Conf., edited by M.E. Bailly and D.E. Sporleder, South Bend, Indiana, USA, p. 267-281.

van der Pluijm, R., Rutten, H.S., Schiebroek, C.S. (1995) - Flexural behavior of masonry in different directions, in: Proc. Fourth. Int. Mas. Conf., London, UK, p. 117-123.

Ryder, J.F. (1963) - The use of small brickwork panels for testing mortars, Trans. Brit. Ceram. Soc., 62.

Samarasinghe, W., Hendry, A.W. (1980) - The strength of brickwork under biaxial tensile and compressive stress, Proc. 7th Int. Symp. on Load Bearing Brickwork, London, UK, p. 129-140.